Spontaneously magnetized Tomonaga-Luttinger liquid in frustrated quantum antiferromagnets

Shunsuke C. Furuya and Thierry Giamarchi
DPMC-MaNEP, University of Geneva, 24 Quai Ernest-Ansermet CH-1211 Geneva, Switzerland

(Received 11 March 2014; revised manuscript received 7 May 2014; published 27 May 2014)

We develop a theory of spontaneously magnetized Tomonaga-Luttinger (TLL) liquid in geometrically frustrated quasi-one-dimensional quantum magnets by taking an $S = 1/2$ ferrimagnet on a union-jack lattice as an example. We show that a strong frustration leads to a spontaneous magnetization because of the ferrimagnetic nature of lattice. Due to the ferrimagnetic order, the local magnetization has an incommensurate oscillation with the position. We show that the spontaneously magnetized TLL is smoothly connected to the existence of a Nambu-Goldstone boson in the canted ferrimagnetic phase of a two-dimensional frustrated antiferromagnet.

DOI: 10.1103/PhysRevB.89.205131 PACS number(s): 75.10.Jm, 75.30.Kz, 75.50.Gg

I. INTRODUCTION

Spontaneous symmetry breaking is one of the most fundamental concepts in physics. It provides the mechanism to generate mass of elementary particles and allows macroscopic alignment of magnetic moments in ferromagnets. Spontaneous breaking of global continuous symmetry is accompanied by a massless excitation, the Nambu-Goldstone boson [1–3]. Since Nambu-Goldstone boson governs low-energy physics at long distance and the low-energy physics is affected by the geometry of system, the dimensionality of the system has strong influences on Nambu-Goldstone boson.

Such effects are most prominent in one dimension (1D) because of the large suppression of ordering at finite temperatures [4,5] and even at zero temperature [6] due to quantum effects. As a result the breaking of a continuous symmetry in 1D is deemed impossible. For systems such as a 1D superfluid, indeed no long-range order exists, and the proper description is the one of a Tomonaga-Luttinger liquid (TLL) [7]. Despite the absence of the true long-range order [8,9], Goldstone modes exist and have a dynamical origin [10]. However, in some rare cases, such as a ferromagnet, the ground state can, even in 1D spontaneously break a continuous symmetry. This prompts immediately for the question of why and for which systems such phenomena can occur.

In order to shed light on the possibility of spontaneous symmetry breaking in 1D, dynamical aspects of the system need to be carefully considered. In addition, in view of the recent experimental progresses in realizing 1D quantum liquids in various situations [11–14], it is worthwhile to search for novel manifestations of spontaneous symmetry breaking in 1D.

For quantum magnetism in 1D, one expects a system with quasi-long-range antiferromagnetic order to have a relativistic dispersion, which is the case of the TLL, while a ferromagnet would have a quadratic one. This behavior of the Nambu-Goldstone boson has been formulated in a quite general context [15–17]. Finding in 1D a system that would spontaneously break the continuous rotational symmetry of the spins, while at the same time retaining some TLL behavior, would thus be interesting and an example of the more general character of Nambu-Goldstone boson.

A very good possibility to realize such a spontaneously magnetized TLL (SMTLL) is offered by ferrimagnetic systems. Several numerical studies [18–24] have followed this route and found incommensurate ferrimagnetic phases which can be candidates for the SMTLL. However, besides the numerical results, there is still no microscopic theory that explains the nature of the incommensurate phase and could relate it to a SMTLL.

In this paper, we present such a theory of the SMTLL, showing that one can have simultaneously a spontaneous breaking of the spin-rotation symmetry leading to a finite magnetization and a TLL behavior. We demonstrate that this SMTLL phase is realized in the ground state of an $S = 1/2$ geometrically frustrated quantum antiferromagnet on a 1D array of the union-jack lattice [see Fig. 1(a)].

II. INSTABILITY OF THE TOMONAGA-LUTTINGER LIQUID

We consider the union-jack (UJ) spin Hamiltonian,

$$\begin{aligned}\mathcal{H} &= J_1 \sum_j \sum_{a=1}^{3} \boldsymbol{S}_{j,a} \cdot \boldsymbol{S}_{j+1,a} + J_1 \sum_j \boldsymbol{S}_{j,2} \cdot (\boldsymbol{S}_{j,1} + \boldsymbol{S}_{j,3}) \\ &\quad + J_2 \sum_j \boldsymbol{S}_{2j,2} \cdot (\boldsymbol{S}_{2j-1,3} + \boldsymbol{S}_{2j+1,1}) \\ &\quad + \alpha J_2 \sum_j \boldsymbol{S}_{2j,2} \cdot (\boldsymbol{S}_{2j-1,1} + \boldsymbol{S}_{2j+1,3}), \qquad (1)\end{aligned}$$

where $J_{1,2} > 0$ and $0 < \alpha \ll 1$. The parameter α denotes the imbalance of the diagonal interactions. Throughout the paper, we fix α and change the ratio J_2/J_1 from 0 to $+\infty$. Note that this model has *a priori* full spin-rotational symmetry.

A. Classical ground state

We first consider the classical ground state minimizing the energy of a unit cell. The classical analysis on the UJ ladder (1) is similar to the 2D UJ antiferromagnet [25–27]. For $0 \leqslant J_2/J_1 < 1/2$, the classical ground state is the Néel state. For $1/2 < J_2/J_1$, spins on the filled sites in Fig. 1(a) become canted with a polar angle $\vartheta = \cos^{-1}(J_1/2J_2)$ and the classical ground state in the canted phase has an incommensurate magnetization,

$$\langle S_{j,a}^z \rangle = \frac{\hbar S}{2}\left(1 - \frac{J_1}{2J_2}\right).$$

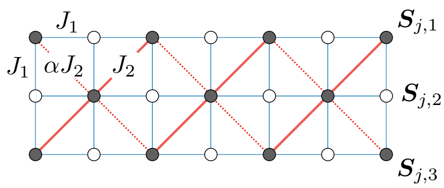

FIG. 1. (Color online) The three-leg union-jack ladder (1).

Hereafter we use $\hbar = 1$ for simplicity. At the classical level, a spontaneous magnetization occurs. However, since quantum fluctuation usually destroys long-range order in 1D systems (1), we have to take them into account to conclude on the existence of a spontaneous magnetization in 1D.

B. The Tomonaga-Luttinger liquid

To do so we derive the low-energy effective field theory of the UJ ladder (1). When the diagonal interaction is small enough, $J_2/J_1 \ll 1$, the low-energy effective field theory is written as a function of two slowly varying fields,

$$\boldsymbol{n} = \frac{1}{2S}\sum_{a=1}^{3}(\boldsymbol{S}_{2j+2-a,a} - \boldsymbol{S}_{2j+3-a,a}), \tag{2}$$

$$\boldsymbol{l} = \frac{1}{2a_0}\sum_{a=1}^{3}(\boldsymbol{S}_{2j+2-a,a} + \boldsymbol{S}_{2j+3-a,a}). \tag{3}$$

Here a_0 is the lattice spacing. We take a diagonal unit cell (Fig. 2) to define $\boldsymbol{n}$ and $\boldsymbol{l}$ along the J_2 bond [28]. The $\boldsymbol{n}$ and $\boldsymbol{l}$ fields denote, respectively, staggered and uniform magnetization densities and satisfy the constraints

$$f(\boldsymbol{n},\boldsymbol{l}) \equiv \boldsymbol{n}^2 - 1 - \frac{1}{S} - \frac{\boldsymbol{l}^2}{S^2} = 0 \tag{4}$$

and $\boldsymbol{n}\cdot\boldsymbol{l} = 0$. The constraint (4) is usually replaceable to $\boldsymbol{n}^2 = 1$. However, the $\boldsymbol{l}^2$ term will play an essential role for our purpose.

The Hamiltonian (1) in the low-energy limit is given by

$$\begin{aligned}\mathcal{H} &= \int \frac{dx}{2}\left[\frac{1}{\sum_{a,b}\mathcal{M}^{-1}_{a,b}}\boldsymbol{l}^2 + 2S^2\sum_a p_a(\partial_x\boldsymbol{n})^2 \right.\\ &\quad \left. + \frac{2S\sum_{a,b}p_a\mathcal{M}^{-1}_{a,b}}{\sum_{a,b}\mathcal{M}^{-1}_{a,b}}(\boldsymbol{l}\cdot\partial_x\boldsymbol{n} + \partial_x\boldsymbol{n}\cdot\boldsymbol{l})\right] \qquad (5)\\ &= \int dx\left[\frac{gv}{2}\left(\boldsymbol{l} - \frac{\Theta}{4\pi}\partial_x\boldsymbol{n}\right)^2 + \frac{v}{2g}(\partial_x\boldsymbol{n})^2\right], \qquad (6)\end{aligned}$$

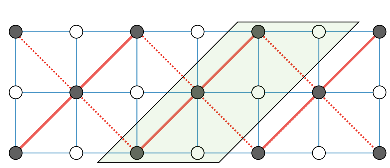

FIG. 2. (Color online) The shaded area depicts the unit cell of the O(3) nonlinear σ model.

where g is a coupling constant, v is the velocity, Θ is a topological angle given by

$$g = \frac{1}{S}\left[2\sum_{a,b,c}p_a\mathcal{M}^{-1}_{b,c} - \left(\frac{\Theta}{4\pi S}\right)^2\right]^{-1/2}, \tag{7}$$

$$v = Sa_0\left[\frac{2\sum_a p_a}{\sum_{b,c}\mathcal{M}^{-1}_{b,c}} - \left(\frac{\Theta}{4\pi S}\frac{1}{\sum_{a,b}\mathcal{M}^{-1}_{a,b}}\right)^2\right]^{1/2}, \tag{8}$$

$$\Theta = 6\pi S, \tag{9}$$

and $p_a = 3J_1/2 + (J_1/2)\delta_{a,2}$. While g and v depend on a 3×3 matrix of microscopic parameters,

$$\mathcal{M} = \begin{pmatrix} 5J_1 - \tilde{J}_2 & J_1 - \tilde{J}_2 & 0 \\ J_1 - \tilde{J}_2 & 6J_1 - 2\tilde{J}_2 & J_1 - \tilde{J}_2 \\ 0 & J_1 - \tilde{J}_2 & 5J_1 - \tilde{J}_2 \end{pmatrix}, \tag{10}$$

with $\tilde{J}_2 = (1+\alpha)J_2/2$, the topological angle (9) is determined only by the number of legs. The derivation of the effective field theory (6) is explained in the case of the three-leg spin ladder in Refs. [28,29]. We obtain the effective field theory (6) by replacing the rung coupling of the three-leg ladder to $J_1 - \tilde{J}_2$ in the matrix (10). We can see from Eq. (5) that information on the structure of the UJ lattice (1) is encoded in the matrix (10). Integrating $\boldsymbol{l}$ out, we obtain [30]

$$\mathcal{H} = \frac{v}{2g}\int dx\left[\frac{1}{v^2}(\partial_\tau\boldsymbol{n})^2 + (\partial_x\boldsymbol{n})^2\right] + i\Theta Q, \tag{11}$$

where $\boldsymbol{n}^2 = 1$ and

$$Q = \frac{1}{4\pi}\int_{-\infty}^{\infty} dx\, \boldsymbol{n}\cdot\partial_\tau\boldsymbol{n}\times\partial_x\boldsymbol{n}$$

gives an integer after integrating with an imaginary time τ; that is, $\int_{-\infty}^{\infty}d\tau\, Q \in \mathbb{Z}$. The Hamiltonian (11) is the $O(3)$ nonlinear σ model (NLSM). The Θ term controls the low-energy limit of the NLSM (11) [31]. When $\Theta \equiv \pi \pmod{2\pi}$, namely when S is a half integer, the $O(3)$ NLSM (11) is identical to the TLL as a conformal field theory with a central charge $c = 1$ [32],

$$\mathcal{H} = \frac{v}{2\pi}\int dx\left[K(\partial_x\theta)^2 + \frac{1}{K}(\partial_x\phi)^2\right]. \tag{12}$$

We use here the notation for the TLL of Ref. [7]. The nature of the ϕ and θ fields will be discussed in detail later. Since Θ is independent of J_2, for small enough J_2, the diagonal interaction is irrelevant and the UJ ladder (1) has the TLL ground state (12), and thus, in particular, zero spontaneous magnetization.

C. Instability at $k = 0$

However, the diagonal interaction has a serious impact on the ground state, and lead to an instability of the TLL. The diagonal interaction J_2 partly compensates J_1 in the matrix (10) and it reduces the velocity down to $v = 0$, where the linearization of the dispersion relation $\omega = vk$ becomes invalid. Let us denote the instability point as J_2^{c1}. The instability point is determined from the zeros of the matrix (10). The matrix $\mathcal{M}$ is positive definite for $\tilde{J}_2 = 0$. As we increase

$\tilde{J}_2$, the positive definiteness first breaks down at $\tilde{J}_2 = 7J_1/3$, namely,

$$J_2^{c1} = \frac{14J_1}{3(1+\alpha)}. \tag{13}$$

When $0 < J_2^{c1} - J_2 \ll J_1$, g and v can be expanded with respect to $(J_2^{c1} - J_2)/J_1$. In fact, since $\sum_{a,b} \mathcal{M}_{a,b}^{-1} \sim [(J_2 - J_2^{c1})/J_1]^{-1}$, we obtain $g \propto S^{-1}[(J_2^{c1} - J_2)/J_1]^{1/2}$ and

$$v \propto J_1 S \left(\frac{J_2^{c1} - J_2}{J_1}\right)^{1/2}. \tag{14}$$

We can easily see that the velocity (14) approaches zero when $J_2 \nearrow J_2^{c1}$. Note that the TLL parameter K must be 1/2 to ensure that the Hamiltonian (12) preserves the $SU(2)$ rotational symmetry [7]. Thus, the susceptibility $\chi = K/\pi v$ of the TLL (12) diverges as $J_2 \nearrow J_2^{c1}$.

Near the instability point $J_2 = J_2^{c1}$, a careful treatment of the interaction is required. The interaction of the $O(3)$ NLSM (11) is nonperturbatively included in the constraint (4). Namely, the partition function Z of the $O(3)$ NLSM (11) is given as a path integral,

$$Z = \int \mathcal{D}\boldsymbol{n}\mathcal{D}\boldsymbol{l}\,\delta(f(\boldsymbol{n},\boldsymbol{l}))\delta(\boldsymbol{n}\cdot\boldsymbol{l}) \exp\left(-\int d\tau \mathcal{H}\right). \tag{15}$$

The constraint (4) generates a strong repulsion $\lambda(\boldsymbol{l}^2)^2$. Indeed, one can add a strongly repulsive interaction $U\{f(\boldsymbol{n},\boldsymbol{l})\}^2$ with $U \nearrow +\infty$ to the Hamiltonian (6) instead of imposing the constraint (4). Then, the partition function (15) is approximated as

$$\begin{aligned} Z &= \int \mathcal{D}\boldsymbol{n}\mathcal{D}\boldsymbol{l}\,\delta(\boldsymbol{n}\cdot\boldsymbol{l}) \exp\left(-U\int d\tau dx \{f(\boldsymbol{n}\cdot\boldsymbol{l})\}^2\right) \\ &\quad \times \exp\left(-\int d\tau \mathcal{H}\right) \\ &= \int \mathcal{D}\boldsymbol{n}\mathcal{D}\boldsymbol{l}\,\delta(\boldsymbol{n}\cdot\boldsymbol{l}) \exp\left(-\int d\tau \bar{\mathcal{H}}\right), \end{aligned} \tag{16}$$

where we obtain the Hamiltonian $\bar{\mathcal{H}}$ with the effective repulsion,

$$\bar{\mathcal{H}} = \int dx \left[\frac{gv}{2}\boldsymbol{L}^2 + \lambda(\boldsymbol{L}^2)^2 + \frac{v}{2g}(\partial_x \boldsymbol{n})^2 + U(\boldsymbol{n}^2 - 1)^2\right], \tag{17}$$

where $\lambda = U/S^4 > 0$ and

$$\boldsymbol{L} \equiv \boldsymbol{l} - \frac{\Theta}{4\pi}\partial_x \boldsymbol{n}. \tag{18}$$

We introduced the quartic interaction $(\boldsymbol{L}^2)^2$ instead of $(\boldsymbol{l}^2)^2$ because their difference (e.g., $\{(\partial_x \boldsymbol{n})^2\}^2$) is negligible, as we see below.

When $J_2 > J_2^{c1}$, the following inequalities are valid:

$$gv = \frac{1}{\sum_{a,b} \mathcal{M}_{a,b}^{-1}} < 0, \tag{19}$$

$$\frac{v}{g} = 2S^2 \sum_a p_a - \left(\frac{\Theta}{4\pi}\right)^2 \frac{1}{\sum_{a,b} \mathcal{M}_{a,b}^{-1}} > 0. \tag{20}$$

Thus, the interaction that the $\boldsymbol{L}$ field feels takes a form of the wine bottle:

$$\frac{gv}{2}\boldsymbol{L}^2 + \lambda(\boldsymbol{L}^2)^2 = \lambda\left(\boldsymbol{L}^2 - \frac{1}{\lambda|gv|}\right)^2 + \text{const.} \tag{21}$$

The potential (21) leads to a nonvanishing expectation value of $\boldsymbol{L}$. Note that the instability occurs only in the uniform part of the $O(3)$ NLSM (17) because of the inequalities (19) and (20). The diagonal coupling only changes the sign of the coupling constant of the $\boldsymbol{L}^2$ [Eq. (19)], keeping that of $(\partial_x \boldsymbol{n})^2$ positive [Eq. (20)]. Namely, the instability only occurs at the wave number $k = 0$ and the nonzero expectation value of the $\boldsymbol{L}$ field (18) is attributed to the magnetization density $\boldsymbol{l}$. Therefore, the ground state has a *spontaneous magnetization* per site, $\boldsymbol{M} \equiv \langle \boldsymbol{l} \rangle/3$, with

$$|\boldsymbol{M}| = \frac{1}{3}\left(\frac{1}{\lambda|gv|}\right)^{1/2} \propto \left(\frac{J_2 - J_2^{c1}}{J_1}\right)^{1/2}. \tag{22}$$

The transition around J_2^{c1} is described by a Ginzburg-Landau-like theory of second-order transitions. Contrarily to the $(\boldsymbol{L}^2)^2$ term, the higher-order interaction $\{(\partial_x \boldsymbol{n})^2\}^2$ is negligible because the lower-order term $(\partial_x \boldsymbol{n})^2$ is stable. Since $\lambda > 0$ the transition cannot be first order. We emphasize that our derivation of the spontaneous magnetization (22) fully respects the $SU(2)$ rotational symmetry and $\boldsymbol{M}$ can point in an arbitrary direction.

D. Nambu-Goldstone bosons

Let us explain the nature of Nambu-Goldstone boson generated from this phase transition. First we focus on the $k = 0$ part. We rewrite the Hamiltonian in terms of fluctuation

$$\boldsymbol{m} \equiv \boldsymbol{L} - 3\boldsymbol{M}. \tag{23}$$

We can assume $\boldsymbol{M} = M(0\,0\,1)^T$ without loss of generality. The longitudinal component m^z has a mass $\Delta = 12\lambda M^2$ because of the interaction (21), that is, $\lambda(\boldsymbol{L}^2 - 9M^2)^2 \simeq 12\lambda M^2(m^z)^2$. The transverse component $\boldsymbol{m}^\perp \equiv (m^x, m^y, 0)$ is the Nambu-Goldstone boson generated from the spontaneous magnetization and it possesses a nonrelativistic dispersion relation [33,34]. Dispersion relations of the longitudinal and the transverse modes are, respectively,

$$E_\parallel(k) = \Delta + \frac{k^2}{2m_\parallel}, \quad E_\perp(k) = \frac{k^2}{2m_\perp}. \tag{24}$$

We can find another massless excitation near $k = \pi$. Then the Hamiltonian (17) turns into

$$\bar{\mathcal{H}} = \int dx \left[4\lambda M^2 \boldsymbol{m}^2 + \frac{v}{2g}(\partial_x \boldsymbol{n})^2\right] + \mathcal{H}'. \tag{25}$$

The repulsion $U(\boldsymbol{n}^2 - 1)^2$ is transformed into the constraint $\boldsymbol{n}^2 = 1$ again. The last term of Eq. (25) denotes the anisotropy that the spontaneous magnetization induces,

$$\mathcal{H}' = V \int dx \{2(m^z)^2 - (m^x)^2 - (m^y)^2\}, \tag{26}$$

with $V = 4\lambda M^2$, which seemingly equals to the coupling constant of $\boldsymbol{m}^2$. However, after including renormalization due to irrelevant operators, the coupling constant V of the anisotropic interaction (26) actually deviates from that of the isotropic part $\boldsymbol{m}^2$. Here we first omit the anisotropy (26) and include it later perturbatively because it does not modify qualitative features of the effective Hamiltonian of the Nambu-Goldstone boson. Let us rewrite Hamiltonian (25) in terms of $\boldsymbol{n}$ and $\boldsymbol{l}$,

$$\bar{\mathcal{H}} = \int dx\left[\frac{\bar{g}u}{2}\left(\boldsymbol{l} - \frac{\Theta}{4\pi}\partial_x\boldsymbol{n}\right)^2 + \frac{u}{2\bar{g}}(\partial_x\boldsymbol{n})^2 - 3\bar{g}u\boldsymbol{M}\cdot\boldsymbol{l}\right]. \tag{27}$$

Here we introduced the coupling constant $\bar{g}$ and the velocity u in a parallel manner as Eq. (6). They are given by

$$\bar{g} = \frac{2M}{S}\left[2\lambda\sum_a p_a - \left(\frac{\Theta}{4\pi S}\right)^2\frac{\lambda}{\sum_{a,b}\mathcal{M}^{-1}_{a,b}}\right]^{-1/2}, \tag{28}$$

$$u = 2MSa_0\left[2\lambda\sum_a p_a - \left(\frac{\Theta}{4\pi S}\right)^2\frac{\lambda}{\sum_{a,b}\mathcal{M}^{-1}_{a,b}}\right]^{1/2}. \tag{29}$$

Note that both $\bar{g}$ and u are positive and proportional to the magnitude of the spontaneous magnetization $|\boldsymbol{M}|$.

The last term of the Hamiltonian (27) can be seen as the Zeeman energy $-\boldsymbol{h}_{\rm eff}\cdot\boldsymbol{S}_{j,l}$. For further understanding of the effective Hamiltonian (27) of the Nambu-Goldstone boson at $k=\pi$, we integrate $\boldsymbol{l}$ out,

$$\bar{\mathcal{H}} = \frac{u}{2\bar{g}}\int dx\left[\frac{1}{u^2}(\partial_\tau\boldsymbol{n} + i\boldsymbol{h}_{\rm eff}\times\boldsymbol{n})^2 + (\partial_x\boldsymbol{n})^2\right] + 9\bar{g}u\int dx\,(\boldsymbol{M}\cdot\boldsymbol{n})^2 + i\Theta Q, \tag{30}$$

where $\boldsymbol{h}_{\rm eff}$ is written as

$$\boldsymbol{h}_{\rm eff} = 3\bar{g}u\boldsymbol{M}. \tag{31}$$

If we include the perturbation $\mathcal{H}'$ at lowest order, it gives a correction

$$\mathcal{H}' \simeq V\int dx(\boldsymbol{M}\cdot\boldsymbol{n})^2[3(n^z)^2 - 1] \tag{32}$$

to the Hamiltonian (30). If we use the value $V = 4\lambda M$, $\mathcal{H}'$ replaces the term $9\bar{g}u(\boldsymbol{M}\cdot\boldsymbol{n})^2 = 9\bar{g}uM^2(n^z)^2$ of Eq. (30) with $27\bar{g}uM^2(n^z)^4$, which has no impact on qualitative aspects of the effective field theory (30).

The $O(3)$ NLSM (30) leads to three important consequences. First, the spontaneous magnetization $\boldsymbol{M}$ leaves $\Theta\equiv\pi \pmod{2\pi}$ intact. Second, $\boldsymbol{M}$ generates the easy-plane anisotropy. Finally, the $O(3)$ NLSM (30) is semiclassical. While the NLSM (11) in the TLL phase has a coupling $g\propto 1/S$, the NLSM (30) has $\bar{g}\propto M/S$ [see Eq. (28)]. Thus, the NLSM (30) behaves similarly to a spin-$S_{\rm eff}$ Heisenberg antiferromagnetic chain with a large half-integer spin $S_{\rm eff}\sim S/M$.

The effective field theory at $k=\pi$ is thus the TLL under an effective magnetic field $\boldsymbol{h}_{\rm eff} = h_{\rm eff}(0\,0\,1)^T$; that is,

$$\bar{\mathcal{H}} = \frac{u}{2\pi}\int dx\left[\bar{K}(\partial_x\theta)^2 + \frac{1}{\bar{K}}(\partial_x\phi)^2\right] - \frac{h_{\rm eff}}{\pi}\int dx\,\partial_x\phi, \tag{33}$$

which is the effective model for the SMTLL. The TLL parameter $\bar{K}$ is determined from the relation [7]

$$M = \frac{h_{\rm eff}\bar{K}}{\pi u}. \tag{34}$$

The TLL parameter

$$\bar{K} = \frac{\pi}{\bar{g}} \propto \left(\frac{J_2 - J_2^{c1}}{J_1}\right)^{-1/2} \tag{35}$$

diverges at the instability point J_2^{c1}. The point J_2^{c1} brings about a divergence of the susceptibility,

$$\chi \propto \left(\frac{|J_2^{c1} - J_2|}{J_1}\right)^{-\gamma}, \tag{36}$$

with the critical exponent γ is given by $\gamma = 1/2$ for $J_2\nearrow J_2^{c1}$ and $\gamma = 1$ for $J_2 \searrow J_2^{c1}$.

E. Dynamical structure factors

We now use this theory to compute the dynamical structure factors in the SMTLL phase. We focus on longitudinal and transverse dynamical structure factors, $S^{\parallel}(k,\omega) = \int_{-\infty}^{\infty} dtdx\, e^{i(\omega t - kx)}\langle S_j^z(t)S_0^z(0)\rangle$ and $S^{\perp}(k,\omega) = \int_{-\infty}^{\infty} dtdx\, e^{i(\omega t - kx)}\langle S_j^+(t)S_0^-(0)\rangle$.

The longitudinal and transverse dynamical structure factors near $k=\pi$ are the same as those of the $S=1/2$ Heisenberg antiferromagnetic chain under magnetic field [7,35],

$$S^{\parallel}[k = \pi(1-2M)+\delta k,\omega] = \frac{\pi^2 C_{\parallel}}{u\Gamma^2(\bar{K})}\theta_H(\omega - u|\delta k|)\left[\frac{4u^2}{\omega^2 - u^2(\delta k)^2}\right]^{1-\bar{K}}, \tag{37}$$

$$S^{\perp}(k = \pi+\delta k,\omega) = \frac{\pi^2 C_{\perp}}{u\Gamma^2\left(\frac{1}{4\bar{K}}\right)}\theta_H(\omega - u|\delta k|)\left[\frac{4u^2}{\omega^2 - u^2(\delta k)^2}\right]^{1-1/4\bar{K}}. \tag{38}$$

$\theta_H(z)$ is the Heaviside's step function and $C_{\parallel}$ and $C_{\perp}$ are nonuniversal constants. Equations (37) and (38) hold when $|\delta k|\ll 1$. The dynamical structure factor near $k=0$ is given by

$$S^{\nu}(k=\delta k,\omega) = \theta_H[\omega - E_\nu(\delta k)]\frac{C'_\nu}{\omega - E_\nu(\delta k)}, \quad (\nu = \parallel, \perp), \tag{39}$$

where $C'_{\parallel}$ and $C'_{\perp}$ are constants. Figure 3 shows the longitudinal and transverse dynamical structure factors in the low-energy region. The dynamical structure factor near $k=0$ (39) clearly shows difference between the SMTLL and either a TLL under magnetic field (e.g., the $S=1/2$ antiferromagnetic chain [7]) or a field-induced TLL (e.g., the $S=1/2$ two-leg spin ladder [36]), for which the symmetry has been externally broken.

III. COMMENSURATE PHASE

A. Commensurability condition

Let us now examine the behavior upon increasing J_2 further. The spontaneous magnetization saturates at a certain point $J_2^{c2}(> J_2^{c1})$. In the case of the UJ ladder, we can find a

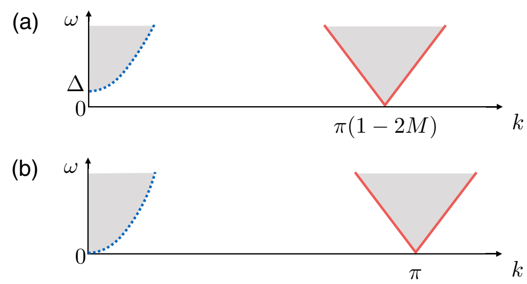

FIG. 3. (Color online) Dynamical structure factors (a) $S^{\parallel}(k,\omega)$ and (b) $S^{\perp}(k,\omega)$ in the low-energy region. Outside of the shaded area, the dynamical structure factor has zero intensity. The red lines represent the linear dispersion of the SMTLL and the blue dashed curves represent the quadratic dispersions (24) of the nonrelativistic Goldstone mode $[E_{\perp}(k)]$ and the massive mode $[E_{\parallel}(k)]$.

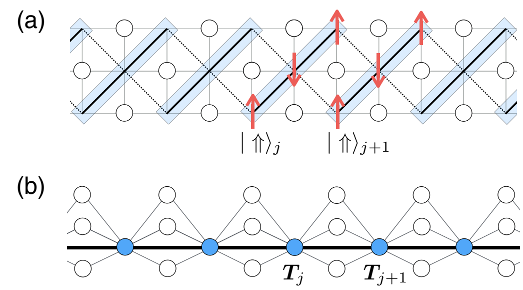

FIG. 4. (Color online) (a) A configuration of trimers (solid rectangles) at $J_2/J_1 \gg 1$. Trimers are surrounded by spins (circles). In the low-energy limit, one can regard the trimer as the $S = 1/2$ pseudospin. The trimer-trimer interaction is ferromagnetic and the trimer-spin interaction is antiferromagnetic. (b) The effective model that describes the commensurate phase. The solid and blank circles represent trimers ($S = 1/2$ pseudospins) and $S = 1/2$ spins, respectively. The thick line represents the ferromagnetic coupling (46) of trimers and the thin lines are the antiferromagnetic coupling of trimers and spins.

saturation condition in the spirit of the Oshikawa-Yamanaka-Affleck theory [37]. To do so, we need to clarify the physical meanings of the ϕ and θ fields of the SMTLL (33). The definitions (2) and (3) of $\boldsymbol{n}$ and $\boldsymbol{l}$ indicate that $\boldsymbol{n}$ and $\boldsymbol{l}$, equivalently ϕ and θ, represent a "center-of-mass" mode. When one considers the UJ ladder (1) as a system of three spin chains weakly coupled by the rung and the diagonal interactions [38], each spin chain is equivalent to a TLL written in a compactified boson ϕ_a and its dual θ_a ($a = 1,2,3$). The bosons ϕ and θ represent the center-of-mass mode because they are given by $\phi = \phi_1 + \phi_2 + \phi_3$ and $\theta = \theta_1 + \theta_2 + \theta_3$. The other "relative-motion" modes, $\phi_1 - \phi_2$ and $\phi_1 + \phi_2 - 2\phi_3$, are massive and negligible in the low-energy effective field theories (12) and (33). The two-site translational symmetry $j \to j + 2$ of the UJ ladder (1) requires the invariance of the effective field theory under the translation

$$\phi \to \phi + 6(S - M)\pi. \tag{40}$$

Given an incommensurate magnetization M satisfying

$$6(S - M) \notin \mathbb{Z}, \tag{41}$$

the incommensurability condition (41) prohibits relevant interactions of ϕ, for instance, $\cos(2\phi)$, to appear in the effective field theory (33). Relevant interactions of θ are not allowed from another reason, that is, the $U(1)$ symmetry of the ground state [37].

Equation (41) shows that the ϕ field can be massive when the incommensurability condition (41) is violated. Increasing M from zero, the condition (41) first breaks down when

$$\frac{M}{M_s} = \frac{1}{3}. \tag{42}$$

Here $M_s = S$ is the saturated value of M. Thus, a commensurate phase as the 1/3 plateau (42) should exist. The commensurate phase has only one massless Nambu-Goldstone boson near $k = 0$ because the SMTLL acquires a mass from a relevant interaction $\cos(2\phi)$. The condition (42) gives the saturation condition of the UJ ladder.

B. Trimer-spin chain

In order to complete the above derivation of the spontaneous magnetization, we show that for large J_2 it can be shown to occur directly from the lattice model (1).

The commensurate phase is identified as a ferromagnetic phase of trimers formed on diagonal J_2 bonds [Fig. 4(a)]. Let us consider the case $J_2/J_1 \gg 1$. When $J_1 = 0$, the UJ ladder (1) is composed of an $S = 1/2$ diamond chain [40,41] and isolated spins. Three spins $\boldsymbol{S}_{2j+1,1}$, $\boldsymbol{S}_{2j,2}$, and $\boldsymbol{S}_{2j-1,3}$ form a trimer [a solid rectangle in Fig. 1(b)] on the strongest J_2 bond. To describe the ground state and the lowest-energy excitation, we may replace the three spins with an $S = 1/2$ pseudospin [41],

$$\boldsymbol{S}_{2j+1,1} = \boldsymbol{S}_{2j-1,3} = \tfrac{2}{3}\boldsymbol{T}_j, \quad \boldsymbol{S}_{2j,2} = -\tfrac{1}{3}\boldsymbol{T}_j. \tag{43}$$

The eigenstates $|\Uparrow\rangle_j$ with $T_j^z = 1/2$ and $|\Downarrow\rangle_j$ with $T_j^z = -1/2$ are written as

$$|\Uparrow\rangle_j = \frac{1}{\sqrt{6}}(|\downarrow\rangle_{j,1}|\uparrow\rangle_{j,2}|\uparrow\rangle_{j,3} - 2|\uparrow\rangle_{j,1}|\downarrow\rangle_{j,2}|\uparrow\rangle_{j,3} + |\uparrow\rangle_{j,1}|\uparrow\rangle_{j,2}|\downarrow\rangle_{j,3}), \tag{44}$$

$$|\Downarrow\rangle_j = \frac{1}{\sqrt{6}}(|\uparrow\rangle_{j,1}|\downarrow\rangle_{j,2}|\downarrow\rangle_{j,3} - 2|\downarrow\rangle_{j,1}|\uparrow\rangle_{j,2}|\downarrow\rangle_{j,3} + |\downarrow\rangle_{j,1}|\downarrow\rangle_{j,2}|\uparrow\rangle_{j,3}). \tag{45}$$

Here $|\uparrow\rangle_{j,a}$ and $|\downarrow\rangle_{j,a}$ are the eigenstates of $S^z_{2j+2-a,a}$ ($a = 1,2,3$). Figure 4(a) depicts that the mapping from spins to a trimer metamorphoses an antiferromagnetic interaction $\alpha J_2 \boldsymbol{S}_{2j,2} \cdot (\boldsymbol{S}_{2j-1,1} + \boldsymbol{S}_{2j+1,3})$ to a *ferromagnetic* trimer-trimer interaction,

$$\alpha J_2 \boldsymbol{S}_{2j,2} \cdot (\boldsymbol{S}_{2j-1,1} + \boldsymbol{S}_{2j+1,3}) = -J_{\mathrm{F}} \boldsymbol{T}_j \cdot \boldsymbol{T}_{j+1}, \tag{46}$$

with $J_{\mathrm{F}} = \frac{4\alpha J_2}{9} + \mathcal{O}(\alpha^2 J_2)$ [41]. Since the trimer-trimer interaction is ferromagnetic, the ground state at $J_1 = 0$ has a nonzero magnetization.

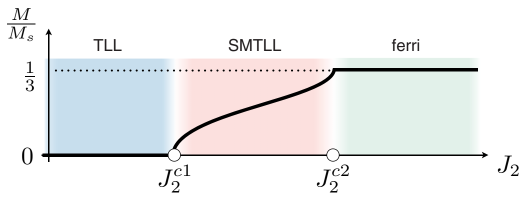

FIG. 5. (Color online) A schematic magnetization curve of the UJ ladder (1). J_2^{c1} and J_2^{c2} represent quantum critical points. The SMTLL phase exists in the region $J_2^{c1} < J_2 < J_2^{c2}$.

At $J_1 = 0$, the residual spins [depicted as blank circles in Figs. 4(a) and 4(b)] are isolated from the trimers. The nonzero J_1 switches on trimer-spin interactions. The low-energy effective Hamiltonian for $J_2/J_1 \gg 1$ is given by

$$\mathcal{H}_{\text{ferri}} = -J_F \sum_{j\in\mathbb{Z}} \boldsymbol{T}_j \cdot \boldsymbol{T}_{j+1} + \sum_{i,j\in\mathbb{Z}} J_{ij} \tilde{\boldsymbol{S}}_i \cdot \boldsymbol{T}_j, \tag{47}$$

where spins not participating in forming trimers are relabeled as $\tilde{\boldsymbol{S}}_j$. Figure 4 (b) shows interactions of the effective model (47). If we are concerned only with the ground-state magnetization of the trimer-spin chain (47), we do not even need the details of coupling constants. We use only three facts, $J_F > 0$, $J_{ij} \geqslant 0$, and $\sum_{l\in\mathbb{Z}} J_{il} > 0$ for $i,j \in \mathbb{Z}$. These conditions enable us to apply the Marshall-Lieb-Mattis theorem [42,43] to the model (47). This theorem imposes that the ground state of the trimer-spin chain (47) must have a fixed magnetization irrespective of parameters J_F and J_{ij}. The ground-state magnetization of the commensurate phase is exactly Eq. (42). Since the ferromagnetic order of the trimer is exactly the ferrimagnetic order of spins, the commensurate phase is exactly the ferrimagnetic phase. Figure 5 shows the ground-state magnetization of the UJ ladder, which reproduces the numerically derived one [24] in the $\alpha = 1$ case. The Marshall-Lieb-Mattis theorem allows us even to take a limit $\alpha \to 1$. However, compared to the numerical result [24], we overestimated J_2^{c1} because of the imbalance $\alpha \ll 1$.

IV. RELATION TO THE GENERAL THEOREM

Now that we have a description of the SMTLL and its Nambu-Goldstone boson, we can compare our result with the general theorem [15–17], claiming that the number of broken generators of the symmetry group determines the number of Nambu-Goldstone boson. The canted phase generally has a nonrelativistic Nambu-Goldstone boson and a relativistic Nambu-Goldstone boson [16,44], which is true in the 2D UJ antiferromagnet [26]. In the 1D case (1), the $U(1)$ symmetry is recovered for the ground state as a result of quantum fluctuations. In the TLL phase, even the full $SU(2)$ symmetry is recovered. Therefore, we conclude that the general theorem [16,17] is applicable to 1D systems at the classical level.

The SMTLL phase results from the competition of the quasi-long-range Néel order of the TLL and the ferrimagnetic order. The geometrical frustration is necessary for the SMTLL to exist because, in the absence of geometrical frustration, the Marshall-Lieb-Mattis theorem prohibits the existence of an incommensurate magnetization (41). However, frustration alone is not sufficient. A frustrated diamond chain [19] has no incommensurate phase. This is because the diamond chain cannot have the TLL and the ferrimagnetic structures simultaneously. By contrast, the UJ ladder is a superposition of the three-leg ladder leading to the TLL and the diamond chain leading to the ferrimagnetic order. In this respect an investigation of itinerant ferrimagnet [45] in 1D would be very interesting.

In conclusion, in this paper, we showed the existence of a spontaneously magnetized phase, with TLL properties, the SMTLL. We gave an effective theory for this phase and computed the magnetization and the dynamical structure factors. We derived the nonrelativistic Nambu-Goldstone boson near $k = 0$ and the SMTLL near $k = \pi$.

ACKNOWLEDGMENTS

We thank T. Shimokawa for giving us the motivation for this study. We are also grateful to M. Oshikawa and H. Watanabe for in-depth discussions. This work is supported by the Swiss National Foundation under MaNEP and division II.

[1] Y. Nambu and G. Jona-Lasinio, Phys. Rev. **122**, 345 (1961).
[2] J. Goldstone, Nuovo Cimento **19**, 154 (1961).
[3] J. Goldstone, A. Salam, and S. Weinberg, Phys. Rev. **127**, 965 (1962).
[4] N. D. Mermin and H. Wagner, Phys. Rev. Lett. **17**, 1133 (1966).
[5] P. C. Hohenberg, Phys. Rev. **158**, 383 (1967).
[6] T. Momoi, J. Stat. Phys. **85**, 193 (1996).
[7] T. Giamarchi, *Quantum Physics in One Dimension* (Oxford University Press, Oxford, UK, 2004).
[8] M. A. Cazalilla, R. Citro, T. Giamarchi, E. Orignac, and M. Rigol, Rev. Mod. Phys. **83**, 1405 (2011).
[9] A. Del Maestro, M. Boninsegni, and I. Affleck, Phys. Rev. Lett. **106**, 105303 (2011).
[10] T. Eggel, M. A. Cazalilla, and M. Oshikawa, Phys. Rev. Lett. **107**, 275302 (2011).
[11] T. Stöferle, H. Moritz, C. Schori, M. Köhl, and T. Esslinger, Phys. Rev. Lett. **92**, 130403 (2004).
[12] J. Taniguchi, Y. Aoki, and M. Suzuki, Phys. Rev. B **82**, 104509 (2010).
[13] M. Klanjšek, H. Mayaffre, C. Berthier, M. Horvatić, B. Chiari, O. Piovesana, P. Bouillot, C. Kollath, E. Orignac, R. Citro, and T. Giamarchi, Phys. Rev. Lett. **101**, 137207 (2008).
[14] M. Jeong, H. Mayaffre, C. Berthier, D. Schmidiger, A. Zheludev, and M. Horvatić, Phys. Rev. Lett. **111**, 106404 (2013).
[15] H. Nielsen and S. Chadha, Nucl. Phys. **105**, B445 (1976).
[16] H. Watanabe and H. Murayama, Phys. Rev. Lett. **108**, 251602 (2012).
[17] Y. Hidaka, Phys. Rev. Lett. **110**, 091601 (2013).
[18] N. B. Ivanov, J. Richter, and U. Schollwöck, Phys. Rev. B **58**, 14456 (1998).

[19] S.-i. Yoshikawa and S. Miyashita, J. Phys. Soc. Jpn. **74**, 71 (2005).
[20] K. Hida, J. Phys.: Condens. Matter **19**, 145225 (2007).
[21] K. Hida and K. Takano, Phys. Rev. B **78**, 064407 (2008).
[22] R. R. Montenegro-Filho and M. D. Coutinho-Filho, Phys. Rev. B **78**, 014418 (2008).
[23] K. Hida, K. Takano, and H. Suzuki, J. Phys. Soc. Jpn. **79**, 114703 (2010).
[24] T. Shimokawa and H. Nakano, J. Korean Phys. Soc. **63**, 591 (2013).
[25] A. Collins, J. McEvoy, D. Robinson, C. J. Hamer, and Z. Weihong, Phys. Rev. B **73**, 024407 (2006).
[26] W. Zheng, J. Oitmaa, and C. J. Hamer, Phys. Rev. B **75**, 184418 (2007).
[27] R. F. Bishop, P. H. Y. Li, D. J. J. Farnell, and C. E. Campbell, Phys. Rev. B **82**, 024416 (2010).
[28] G. Sierra, arXiv:cond-mat/9610057.
[29] G. Sierra, J. Phys. A: Math. Gen. **29**, 3299 (1996).
[30] I. Affleck, J. Phys.: Condens. Matter **1**, 3047 (1989).
[31] F. Haldane, Phys. Lett. A **93**, 464 (1983).
[32] I. Affleck and F. D. M. Haldane, Phys. Rev. B **36**, 5291 (1987).
[33] T. Brauner, Symmetry **2**, 609 (2010).
[34] T. Brauner, Phys. Rev. D **75**, 105014 (2007).
[35] R. Chitra and T. Giamarchi, Phys. Rev. B **55**, 5816 (1997).
[36] P. Bouillot, C. Kollath, A. M. Läuchli, M. Zvonarev, B. Thielemann, C. Rüegg, E. Orignac, R. Citro, M. Klanjšek, C. Berthier, M. Horvatić, and T. Giamarchi, Phys. Rev. B **83**, 054407 (2011).
[37] M. Oshikawa, M. Yamanaka, and I. Affleck, Phys. Rev. Lett. **78**, 1984 (1997).
[38] Strictly speaking, our model (1) is out of scope of such a weak coupling approach. However, it is known that the weak coupling approach still gives qualitatively reasonable results [39] in the TLL phase. As we will see later, this approach is qualitatively valid even in the magnetized phases.
[39] H. J. Schulz, Phys. Rev. B **34**, 6372 (1986).
[40] K. Takano, K. Kubo, and H. Sakamoto, J. Phys.: Condens. Matter **8**, 6405 (1996).
[41] T. Tonegawa, K. Okamoto, T. Hikihara, Y. Takahashi, and M. Kaburagi, J. Phys. Soc. Jpn. **69**(Suppl. A), 332 (2000), arXiv:cond-mat/9912482v1.
[42] W. Marshall, Proc. R. Soc. A **232**, 48 (1955).
[43] E. Lieb and D. Mattis, J. Math. Phys. **3**, 749 (1962).
[44] J. M. Román and J. Soto, Phys. Rev. B **62**, 3300 (2000).
[45] H. Ishizuka and Y. Motome, Phys. Rev. Lett. **109**, 237207 (2012).